

Electronic Supplementary Information

Unraveling the role of solvent–precursor interaction in cooking heteroatomic carbon cathode for high-energy-density Zn-ion storage

Hui Duan,[‡] Ziyang Song,[‡] Ling Miao, Liangchun Li, Dazhang Zhu, Lihua Gan* and Mingxian Liu*

H. Duan, Z. Song, Dr. L. Miao, Prof. L. Li, Prof. D. Zhu, Prof. L. Gan, Prof. M. Liu

Shanghai Key Lab of Chemical Assessment and Sustainability, School of Chemical Science and Engineering, Tongji University, Shanghai, 200092, P. R. China.

*E-mail: ganlh@tongji.edu.cn; liumx@tongji.edu.cn

Experimental Section

Synthesis

2.55 mL glyoxal (0.02 mol), 3.164 g 1, 5-diaminonaphthalene (0.02 mol) and 100 mL solvent (one of water, tetrahydrofuran (THF), dioxane (DOA), *N*-methyl-2-pyrrolidone (NMP), dimethylformamide (DMF), ethanol (EtOH)) was mixed and stirred at 70 °C for 3 h. After filtration, washing and drying, the obtained polymer (termed as GDN) was mixed with potassium hydroxide, and subsequently carbonized at 700 °C for 2 h in N₂ atmosphere to fabricate carbons (denoted as C_{Water}, C_{THF}, C_{DOA}, C_{NMP}, C_{DMF}, and C_{EtOH}).

Characterization

The morphologies of the samples were observed on a Hitachi S-4800 scanning electron microscopy (SEM). The Fourier transform infrared (FT-IR) spectra were examined using a Thermo Nicolet NEXUS spectrometer. Thermogravimetric analysis of the polymers was performed employing a Netzsch STA409 PC analyzer in N₂ flow at a heating rate 10 °C min⁻¹.

X-ray powder diffraction (XRD) analysis was collected by a diffractometer (Bruker D8 advance system) equipped with a Cu K radiation source. Nitrogen sorption measurements were conducted on a Micromeritics ASAP 2460 apparatus at $-196\text{ }^{\circ}\text{C}$. The surface areas were estimated using Braunauer–Emmett–Teller method within the pressure range of $P/P_0=0.05\text{--}0.25$. The pore size distributions were recorded by the nonlocal density functional theory calculations with carbon model of slit pores. Surface functionality was measured by an X-ray photoelectron spectroscopy (XPS) with Al Ka radiation. microscope. Ultraviolet visible near infrared (UV–vis–NIR) spectra were obtained using an Agilent Carry 5000 spectrometer.

Fabrication of C_X -based Zn-ion hybrid supercapacitors

The working electrode was prepared by coating the slurry containing C_X sample, polytetrafluoroethylene and graphite with a mass ratio of 8:1:1 onto the stainless-steel mesh (the mass loading of active substance is $\sim 10\text{ mg cm}^{-2}$). To assemble the Zn-ion hybrid supercapacitors, the Zn foil as anode and the carbon electrode as cathode were packed in a CR2032-type coin cell using $3\text{ mol L}^{-1}\text{ Zn}(\text{SO}_3\text{CF}_3)_2$ as electrolyte.

Electrochemical measurement

A CHI660E electrochemical workstation was employed to investigate the electrochemical performances of the devices including cyclic voltammetry (CV) and electrochemical impedance spectroscopy (EIS). The galvanostatic charge/discharge (GCD) measurement of Zn-ion devices was performed on a LAND-CT3001A system. The specific capacity (C_m), energy density (E) and power density (P) of the devices were obtained based on the following forms:

$$C_m (\text{mAh g}^{-1}) = \frac{I \times \Delta t}{m} \quad (1)$$

$$E (\text{Wh kg}^{-1}) = C_m \times \Delta V \quad (2)$$

$$P (\text{W kg}^{-1}) = \frac{E}{\Delta t} \quad (3)$$

where I (A), Δt (s), m (g), ΔV (V) is the current density, discharge time, mass loading and voltage window, respectively.

Simulation Details

In this study, all the structures (monomer, dimer and solvent molecules) were determined under density functional theory (DFT) method using the Dmol³ program package in Materials Studio 2018. The exchange and correlation terms were determined using the Generalized Gradient Approximation (GGA) in the form proposed by Perdew, Burke, and Ernzerhof (PBE).^[S1] Subsequently, the hirshfeld charge analysis of the optimized structures was carried out. Subsequently, these charged stable structures are applied to dynamics simulation through the Forcite module.

Two polymer chains, each containing eight units, were randomly dissolved in water (1500) and ethanol (1000) using the Amorphous Cell module, respectively. The initial cubic simulation lattice for the two systems was exactly the same with the dimensions ($x=50.0$ Å, $y=48.0$ Å, and $z=48.0$ Å). The simple point charge (SPC) model,^[S2] which can accurately describe the water solution environment,^[S3] is adopted for all water molecules.

All MD simulation were performed using the COMPASS force field,^[S4, S5] which is a force field for atomistic simulation of common organic molecules based on the state-of-the-art ab initio and empirical parametrization techniques.^[3] All simulations were equilibrated at constant temperature (343.15 K) and volume (NVT) for 10 ns. Atomic coordinates were saved for every 50 ps.

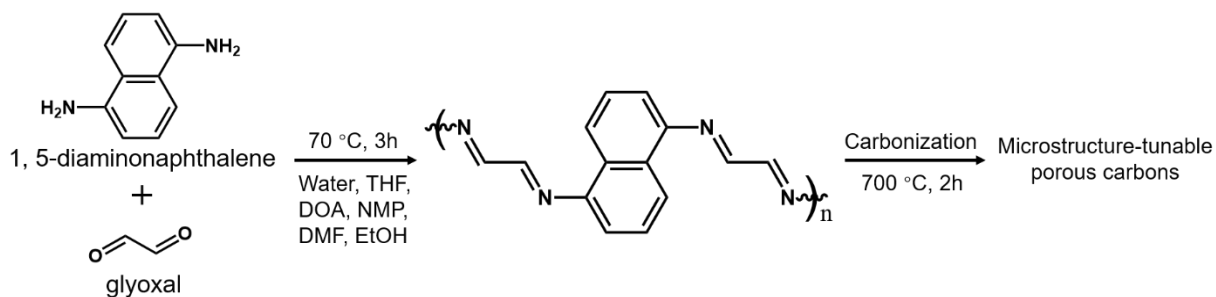


Fig. S1 Schematic synthesis of versatile carbons via a Schiff-base reaction between 1, 5-diaminonaphthalene and glyoxal in different solvents, followed by a carbonization procedure.

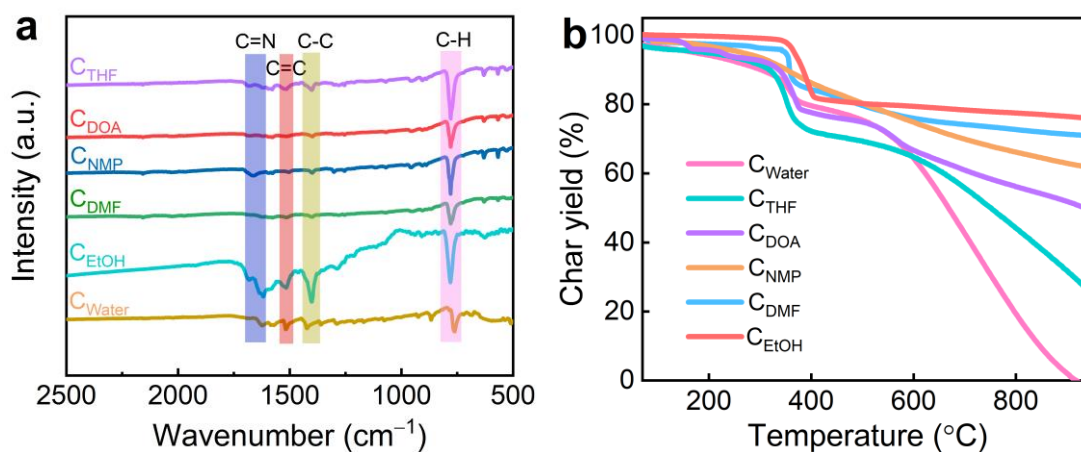


Fig. S2 (a) FI-IR spectra and (b) char yields of the polymer prepared with different solvents.

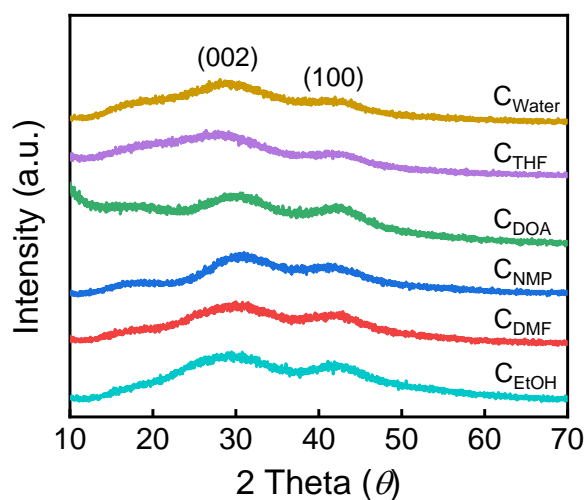


Fig. S3 XRD patterns of the carbons.

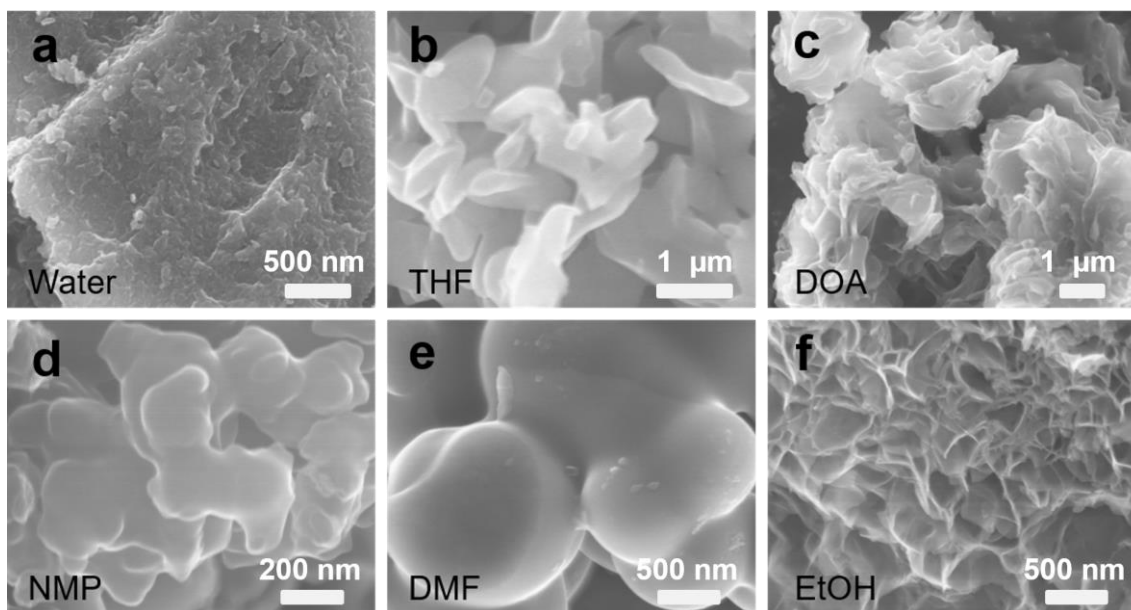


Fig. S4 SEM images of the polymers synthesized using the solvent of (a) water, (b) THF, (c) DOA, (d) NMP, (e) DMF and (f) EtOH.

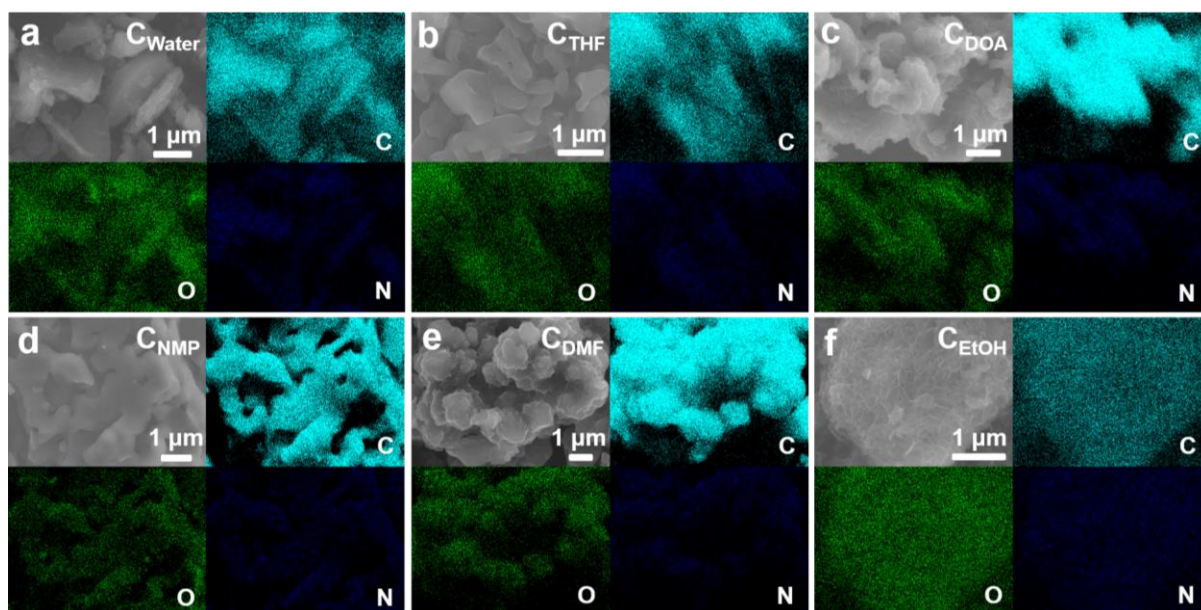


Fig. S5 The element mapping images of C, N and O species for (a) C_{Water} , (b) C_{THF} , (c) C_{DOA} , (d) C_{NMP} , (e) C_{DMF} , and (f) C_{EtOH} .

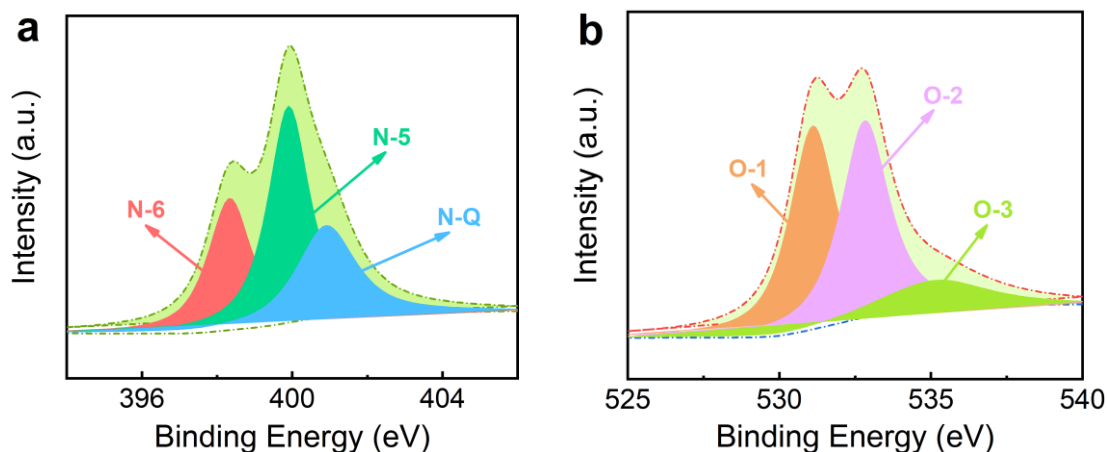


Fig. S6 High-resolution N 1s and O 1s XPS spectra of C_{DMF}.

Calculation of Hansen solubility parameters of the polymers.

The Hansen solubility parameters of the polymers was experimentally estimated through the dissolution strategy based on the literature,^[S6, S7] which were acquired as solubility parameters related to the solvent that exhibit the highest dispersion concentration. Specifically, the 1, 5-diaminonaphthalene/glyoxal polymer was initially sonicated in a wide range of solvents with known δ values to form dispersions. The obtained dispersions were allowed to stand for one day, and the concentrations of polymers in the supernatant of the dispersions were then obtained by the Beer-Lambert-Bouguer law according to the measured absorbance, which was the maximum absorbance of polymers. By this process, the equilibrium concentrations of polymers in each of the twelve solutions with different δ could be obtained. The concentration was plotted vs. the solubility parameters. Based on this approach, the δ of the polymer were experimentally determined.



Fig. S7 Photographs of the polymer dispersed in six experimental solvents.

Table S1. Hansen solubility parameters of twelve solvents used in this work.^[S8]

Order	Solvent	δ_T	δ_D	δ_P	δ_H
1	Hexane	15.3	14.9	0	0
2	Dichloroethane	18.4	16.6	8.2	0.4
3	Tetrahydrofuran	19.5	16.8	5.7	8
4	Acetone	20	15.5	10.4	7
5	Dioxane	20.5	19	1.8	7.4
6	<i>N</i> -methylpyrrolidone	23.1	18.0	12.3	7.2
7	Isopropanol	23.5	17.6	6.1	15.1
8	Dimethylformamide	24.8	17.4	13.7	11.3
9	Ethanol	26.5	15.8	8.8	19.4
10	Dimethyl sulfoxide	26.7	18.4	16.4	10.2
11	Methanol	29.6	15.1	12.3	22.3
12	Water	47.9	15.5	16	42.4

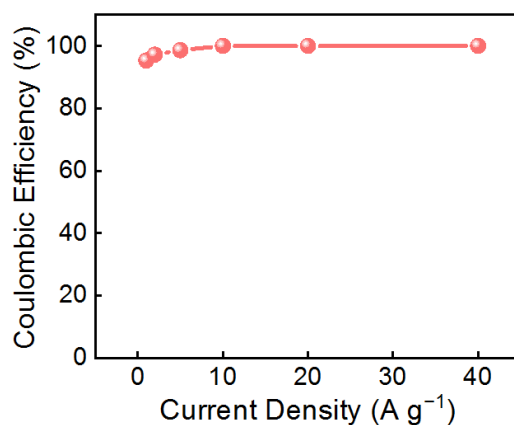


Fig. S8 The trend of Coulombic efficiency with enlarged current density for the fabricated C_{EtOH}-based supercapacitors.

Table S2. Comparison of specific capacity (C_m), mass loading of active materials, energy density (E), and cycle stability of reported Zn-ion carbon-based hybrid supercapacitors in the recent literatures.

Materials	C_m (mAh g ⁻¹)	Mass Loading (mg cm ⁻²)	E (Wh kg ⁻¹)	Lifespan % @cycle@A g ⁻¹	Refs.
C _{EtOH}	170	10	92.8	93.5% @40,000@40	This work
Bio-carbon	94	N/A	52.7	91% @20,000@2	S9
Activated carbon	121	0.7–0.8	84	91% @10,000@1	S10
Carbon spheres	86.8	1.0–1.2	59.7	98% @15,000@1	S11
Layered carbon	127.7	2.0	86.8	81.3% @6,500@5	S12
Carbon sheets	105	0.88	75.22	60% @4,000@1	S13
Activated carbon	231	0.6	77.5	70% @18,000@10	S14
Graphene films	99.3	N/A	76.2	90% @10,000@15	S15
Porous carbon	49.8	1	58.1	100% @9,000@1	S16

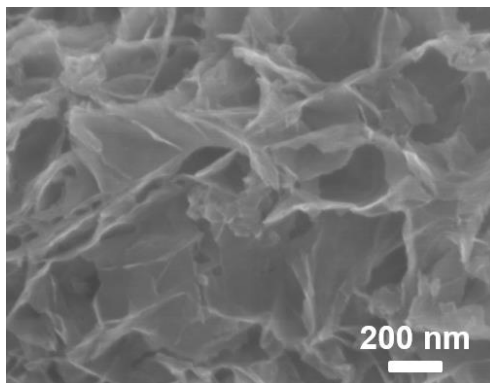


Fig. S9 SEM image of the C_{EtOH} cathode in Zn-ion hybrid supercapacitor after 40000 cycles.

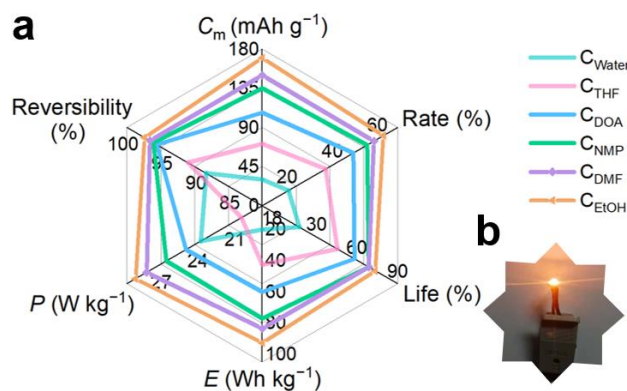


Fig. S10 (a) Comparison chart of six metrics of C_X devices. (b) A LED lamp powered by the C_{EtOH} -based Zn-ion supercapacitor.

Table S3. The comparison of parameters related to ion diffusion kinetics of the devices.

Devices	R_s (Ω)	R_{ct} (Ω)	σ ($\Omega s^{-0.5}$)	D_{H^+} ($cm^2 s^{-1}$) $\times 10^{-9}$
C_{Water}	2.66	78.3	134.6	0.76
C_{THF}	1.95	75.6	86.6	1.18
C_{DOA}	1.97	55.7	77.2	1.33
C_{NMP}	1.32	45.4	37.1	2.76
C_{DMF}	1.15	25.3	32.9	3.11
C_{EtOH}	1.09	15.9	24.2	4.23

References

- S1. J. P. Perdew, K. Burke, M. Ernzerhof, *Phys. Rev. Lett.* **1996**, *77*, 3865.
- S2. H. J. C. Berendsen, J. R. Grigera, T. P. Straatsma, *J. Phys. Chem.* **1987**, *91*, 6269.
- S3. M. J. Wiedemair and T. S. Hofer, *Phys. Chem. Chem. Phys.* **2017**, *19*, 31910.
- S4. H. Sun, *Comput. Theor. Polym. Sci.* **1998**, *8*, 229.
- S5. H. Sun, *J. Phys. Chem. B* **1998**, *102*, 7338.
- S6. H. Launay, C. M. Hansen, K. Almdal, *Carbon* **2007**, *45*, 2859.
- S7. S. Ata, T. Mizuno, A. Nishizawa, C. Subramaniam, D. N. Futaba, K. Hata, *Sci. Rep.* **2014**, *4*, 7232.
- S8. D. J. Hansen C., Kontogeorgis G., Panayiotou C., Williams L., Poulsen T., Priebe H., Redelius P., Boca Raton: CRC Press 2007.
- S9. H. Wang, M. Wang and Y. Tang, *Energy Storage Mater.* **2018**, *13*, 1.
- S10. L. Dong, X. Ma, Y. Li, L. Zhao, W. Liu, J. Cheng, C. Xu, B. Li, Q.-H. Yang, F. Kang, *Energy Storage Mater.* **2018**, *13*, 96.
- S11. S. Chen, L. Ma, K. Zhang, M. Kamruzzaman, C. Zhi, J. A. Zapien, *J. Mater. Chem. A* **2019**, *7*, 7784.
- S12. Y. Lu, Z. Li, Z. Bai, H. Mi, C. Ji, H. Pang, C. Yu and J. Qiu, *Nano Energy* **2019**, *66*, 104132.
- S13. Y. Zhang, Z. Wang, D. Li, Q. Sun, K. Lai, K. Li, Q. Yuan, X. Liu and L. Ci, *J. Mater. Chem. A*, **2020**, *8*, 22874.
- S14. Z. Zhou, X. Zhou, M. Zhang, S. Mu, Q. Liu, Y. Tang, *Small*, **2020**, *16*, 2003174.
- S15. Y. Zhu, X. Ye, H. Jiang, J. Xia, Z. Yue, L. Wang, Z. Wan, C. Jia, X. Yao, *J. Power Sources*, **2020**, *453*, 227851.
- S16. X. Qiu, N. Wang, Z. Wang, F. Wang, Y. Wang, *Angew. Chem. Int. Ed.* **2021**, *60*, 9610.